applied sciences

MDPI

Article

Development of a Pipeline Inspection Robot for the Standard Oil Pipeline of China National Petroleum Corporation

Hui Li [1,2], Ruiqin Li [1,*], Jianwei Zhang [3] and Pengyu Zhang [4]

1 School of Mechanical Engineering, North University of China, Taiyuan 030051, China; lihui@llhc.edu.cn
2 Department of Mining Engineering, Luliang University, Lvliang 033001, China
3 Department of Informatics, University of Hamburg, 22527 Hamburg, Germany; zhang@informatik.uni-hamburg.de
4 Together Foison (Beijing) Technology Co. Ltd., Beijing 100176, China; m17600482344@163.com
* Correspondence: liruiqin@nuc.edu.cn

Received: 1 April 2020; Accepted: 17 April 2020; Published: 20 April 2020

Featured Application: This paper presents a promising solution for the use of a robotic system to remotely perform inspection tasks in the oil pipelines.

Abstract: The periodic inspection for oil pipelines is required due to the deterioration over time. A multitude of factors brings such a deterioration, from corrosion, leaks, to cracks, which may lead to blowbacks and cause the damages for operators and the environments. With the progress of robotics technology, various types of mobile robots and mechanisms are designed to cope with this issue. Rather than the assignment of human workers in hazardous environments, the deployment of such kinds of inspection robots can take on this duty more time-efficiently and safely, preventing the human workers from the high-risk of the inspection task in the oil pipelines. This paper presents a novel design of a mobile robot for oil pipeline inspection, which is cooperated with the China National Petroleum Corporation (CNPC). With the improvement of the previous inspection robot used in CNPC's standard oil pipelines, the newly designed robot is composed of six groups of symmetrical supporting wheels, and a more powerful motors as well as a more advanced control system. This new design endows the oil pipeline inspection robot with better performance on six aspects: traction, obstacle-adaptivity, operation endurance, gradeability, visual perception, and stability. The field testing results at multiple oil transfer stations across several months demonstrate the reliability of this mobile robot under various severe situations in China and validate its performance in the studied aspects.

Keywords: inspection robot; robotic system

1. Introduction

In the past few decades, petroleum has always been one of the most important resources in the progressing of human civilization. For petroleum corporations, the periodic inspection of their oil pipelines is vital, where the deployments of these pipelines are everywhere in oil refineries and oil transfer stations (Figure 1). However, the deterioration of these pipelines cannot be avoided as oil is transported over time. Once the oil pipelines get deterioration, it could bring the owners of these corporations huge economic loss during the processes of oil transportation. Furthermore, the damage is not merely confined to the aspect of the economy. For example, the pipeline corrosion and cracks, which are commonly caused by the impurities in the pipelines, could lead to severe soil/ocean pollution or even explosions.

Figure 1. Deployment of oil pipelines in unstructured environment.

In China, the China National Petroleum Corporation (CNPC) is one of the largest energy corporations that manage the refinement, storage, and transportation of oil products. To operate such a huge business, the CNPC is required to conduct careful maintenance, repair, and operations (MRO) on the deployed facilities, especially the oil pipelines which serve as one of the most important components to connect all the facilities. According to the statistical data of the CNPC, the distance of the deployed pipelines achieves 86,734 (km) in China by the end of 2018 [1]. In particular, about RMB 120 million was invested in the MRO of these pipelines [2]. Therefore, there is a demand for the CNPC to

obtain an effective solution for autonomous inspection with robotic technologies. In such a solution, the developed robot is expected to have the capabilities of stably moving inside various standardized oil pipelines that the CNPC is using. In addition, there are multiple sensors mounted on the robot for the environment inspection and robot state monitoring. The contents of the inspection inside the oil pipelines includes the ID of pipelines, the completeness of welding seam lines of pipelines, the existence of water stains, the coverage of anticorrosive layers, etc. Through the fully deployed technology of 5G in the near future, the robot will be able to be operated remotely by skilled workers—or operated autonomously—for a comprehensive inspection of the oil pipelines and upload the inspection results for timely analysis. The CNPC believes that the deployment of this robot will not only guarantee the safety of the on-site inspection workers but also improve the efficiency of the diagnosis on their facilities, enabling an instant alert if faults occur.

For the requirements from CNPC, the robot is expected to have a nontowline design that can operate under its self-power and support a cruising range of 60 (km) for every inspection task. Due to the moisture and dust inside the oil pipelines, the IP ratings should be better than IP67. For the mobility criteria of the robot, the robot can move in an incline with no more than $\pm 45^{\circ}$ and adapt to geometric deformation of 10%, while keeping uniform speed in the standard pipelines of the CNPC ($1219 \leq \phi \leq 1440$ mm). With the installed sensors, the robot can achieve the deformation of pipelines with a precision of ± 1 mm. Besides, the paved road map of the oil pipelines can be mapped simultaneously during the inspection.

To design a robot that fulfills the requirements proposed by the CNPC, some literature is investigated. For external inspection of pipelines, magnetic wheels were employed to enable the robot to attach onto the surfaces of pipelines [3] and storage tank [4,5]. For internal inspection of pipelines, while magnetic wheels can work in such a scene [6,7], a robot with an automatic tractive force adjusting function is more reliable as it enables the robot to actively adapt to the pipeline diameters [8]. Except for the use of wheels, caterpillar [9] and shape memory alloy actuators [10] are also a selection for moving inside pipelines. For the design of inspection robots, a two-module design was employed to perform compliance with the deformation of pipelines [11]. Another design is to provide adaptivity through the use of a steering mechanism inside pipelines [12]. Other designs of the pipeline inspection robots are also worthy for study [13–16]. In addition, many aspects should be carefully considered on the integration of robotic systems, such as intelligence [17,18], perception [19,20], task planning [21], robot control [22–24], fault tolerance [25,26], etc. All these aspects bring challenges to the successful development of robotic systems for oil pipeline inspection.

This paper presents a novel pipeline inspection robot that has satisfied the requirements of the CNPC and basically focuses on the experimental results in this project. The improvements in the new design compared to the previous design that was deployed in the CNPC are analyzed. Besides, the field testing results on six aspects—traction, obstacle-adaptivity, operation endurance, gradeability, visual perception, and stability—are given to provide a comprehensive summary of this product.

2. Design of Mobile Robot

2.1. Previous Design and Challenges

Figure 2 illustrates the previous design of the oil pipeline inspection robot. The inspection robot is composed of three sets of symmetric supporting wheels with two wheels in each set. Each spring mechanism is connected between a fixture and a motion component, with the corresponding numbering, to compose a compliance mechanism that connects each wheel and the chassis. To generate the motion commands for the inspection robot to move inside the pipelines, a Bluetooth signal is sent from a mobile phone before the robot enters the pipelines. During the operation in the pipelines, the robot can perform the inspection and motion control autonomously. The spring mechanisms facilitate the stable motion of the inspection robot when there is an uneven environment inside oil pipelines. Besides, the waterproof charging connector can be used for charging when the robot reaches low battery.

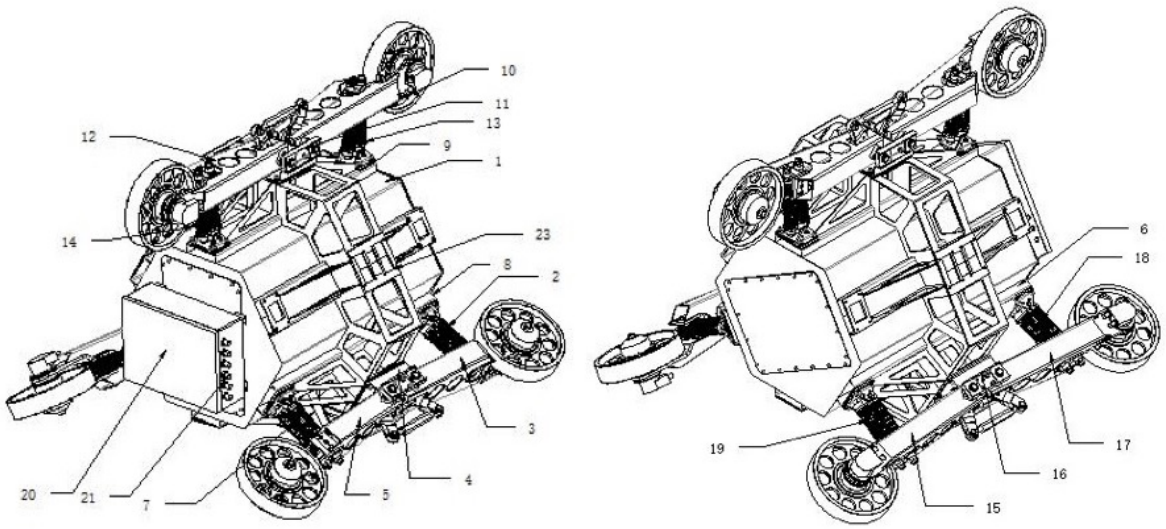

Figure 2. Previous design of oil pipeline inspection robot: (1) power box; (2) spring mechanism No. 1; (3) motion component No. 1; (4) connection component No. 1; (5) motion component No. 2; (6) fixture No. 3; (7) spring mechanism No. 2; (8) fixture No. 1; (9) fixture No. 2; (10) motion component No. 3; (11) connection component No. 2; (12) motion component No. 4; (13) spring mechanism No. 3; (14) spring mechanism No. 4; (15) motion component No. 5; (16) connection component No. 3; (17) motion component No. 6; (18) spring mechanism No. 6; (19) spring mechanism No. 5; (20) control box; (21) waterproof charging connector; (22) battery; (23) chassis.

Figure 3 demonstrates the operation of the previous inspection robot in real scenes. After the on-site deployment for a period, some issues are found:

1. When the robot moves forward in the pipeline, it rotates irregularly in the circumferential direction. Although the compliance mechanisms are used to support the chassis and other components, the excessive force exerted from the rotation leads to the overheat of motors.
2. The power supply systems were powered by a single lithium battery. Under this circumstance, once any set of wheels is damaged due to overheating, the robotic system will be out of control. At this moment, short-circuit causes melting of the connection to the power supply. Then, the robot stops to operate and gets blocked in the pipeline.

Figure 3. Operation scenes of previous inspection robot.

2.2. Improvement

Encountering these issues gave us the inspiration to improve the previous design for better performance during operation. Figure 4 shows the new design of the inspection robot. Based on the previous design, the number of sets of symmetric supporting wheels is increased to six in the new design of the inspection robot. Besides, the power of motors are also upgraded. In the case that the irregular circumferential rotation occurs, at least two sets of supporting wheels can provide the power, thereby preventing motor damages from the overheat of motors due to excessive loads. On the layout of power supply, the upgraded power supply system of the inspection robot uses separate driving power for each driving wheel, the control system, and the detection system; it also has a backup battery, enabling the inspection robot to return back successfully once any of the power supplies fail.

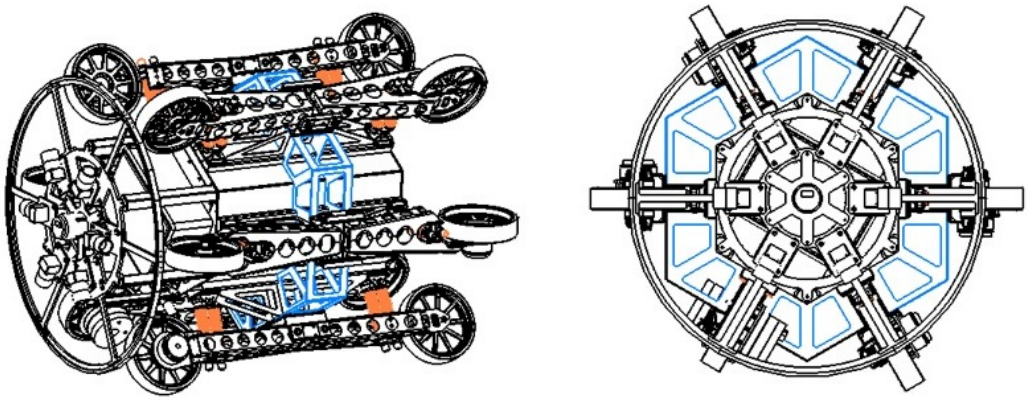

Figure 4. New design of oil pipeline inspection robot.

Figure 5 demonstrates the operation of the new inspection robot in real scenes. In the following section, the detailed design will be given.

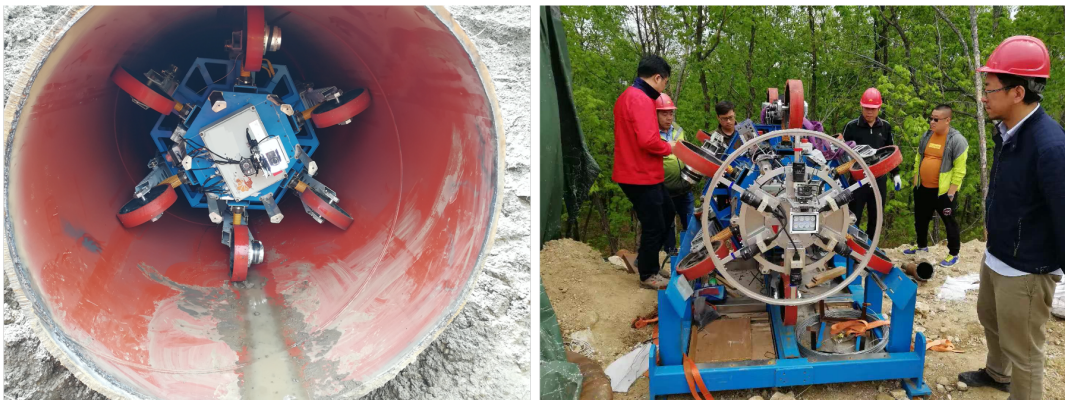

Figure 5. Operation scenes of new inspection robot.

2.3. Mechanical Design

2.3.1. Overall Structure

The overall inspection robot is composed of a power box, supporting arm, driving wheels, control box, etc. The power box is located at the center of the robot, containing a 48-V 400-Ah lithium battery to support the robot's continuous power requirements. Meanwhile, the power box is also the core for connecting other components. The cover of the power box is made of stainless steel (SUS304, TianJin Lishen Battery Joint-Stock CO., LTD., Tianjin, China), where each sheet metal is combined with full welding to ensure the mechanical strength and waterproof performance of the entire power box.The supporting arm is connected to the power box through a rotating shaft, where the damping of

the supporting arm is achieved by a rectangular coil spring to ensure sufficient compression stroke and minimal deformation force. Each driving wheel is driven directly by motor; while this design has the same kinematic properties as the nonintegrated drive system, it has a smaller weight and transmission resistance, thus increasing the cruising range. The control box adopts an explosion-proof and waterproof cover, where there is a microcontroller and other related main circuits installed inside. The high-definition camera units are externally attached to the end of the power box, which aims to record the conditions inside oil pipelines. After the inspection is completed, the captured images are processed manually for defect inspection. The laser detection device is externally attached to another end of the power box for recording the geometrical dimensions of the environment. After the detection is completed, the geometrical deformation of pipelines is labeled.

2.3.2. Design of Supporting Arm

The supporting arm is made of high-strength carbon steel laser cutting, CNC sheet metal forming, and spiral bending welding forming. The surface is electrostatically sprayed to ensure the parts are corrosion resistant. The lower side of the supporting arm uses a rectangular coil spring as an elastic element, where the spring has a large compression stroke and a small spring constant, ensuring sufficient passing capacity and small passing resistance. Meanwhile, the buffer device tries to reduce its dimensions to ensure that there is enough space for installation. The device also has a spring strength fine-tuning mechanism to support the adjustment of the supporting force of the buffer device.

2.3.3. Design of Driving Wheels

Each driving wheel uses a harmonic frameless geared motor, where there is no redundant connection used and the size is compact. Besides, the bearing structure of the harmonic reducer ensures that the geared motor can directly bear a large amount of axial and radial forces without an additional shaft system to support the weight of the robot body, which greatly reduces the weight of the driving wheels. The detailed parameters of the used motor are depicted in Table 1. The rated output torque of this motor is 68.48 Nm and the maximum output torque is 121.01 Nm.

Table 1. Parameters of used motor (KAH-25A).

Reduction Ratio	Rate Velocity (rpm)	Rate Current (A)	Max. Current (A)	Torque Const. (Nm)
1 : 51	51	16.19	28.61	4.23

The motor drivers use high-current, low-voltage DC drivers. According to the motor parameters, we chose the drivers' maximum peak current as 70.8 A, which meets the requirements under motor overload conditions. Due to the small size of the used drivers, the integration with the motion controller inherits the functions of advanced motion control and logical control. Besides, the driver supports various types of encoder feedback, providing flexible bus communication protocols and programming environments. Besides, a temperature detection system is employed on the motors, where the used sensor is a PT100 temperature sensor. Each sensor is tightly fixed to each motor body and detects the real-time temperature of the motor. After passing a converter, the resistance signal of PT100 is converted into the RS485 digital signal for postprocessing in the control system.

The hub of each driving wheel is made of aviation aluminum 6063-T4 through CNC machining to ensure the strength of the wheel structure. The wheel surface is made of high-strength polyurethane. Besides, the hub and the wheel surface are combined with a rubber coating process to enhance the bonding. The wheel surface adopts polyurethane material to reduce wheel damage when the robot is moving inside oil pipelines.

2.4. Control System

The control system is composed of a microcontroller, memory card, buzzer, LED indicators, and other auxiliary modules. The microcontroller is STMicroelectronics' STM32 series 32-bit ARM Cortex-M4, which operates at 64 MB. It integrates Flash memory, a clock, 12-bit analog-to-digital conversion, a CAN bus, serial communication, etc. The power circuit plays a vital role in the normal and stable operation of the controller. The input range of the microcontroller's power is between DC 9–30 V. The switching regulator uses the American company's peak buck/boost and reverse-switching-regulator MC33063 (ON Semiconductor Corporation, Phoenix, Arizona, USA). It also supports reverse power protection, overcurrent protection, filtering, and other circuits, ensuring that the entire microcontroller works normally.

To send the commands to the control system remotely, a remote controller is developed, where the wireless communication module is based on the LoRa technology and the communication range is tested to be within 500 m. This range is measured when the controller is at the entrance of the pipelines, where the signal is transmitted to the robot through the refraction and the air inside the pipelines.

2.5. Inspection System

2.5.1. Sensors

The inspection system uses 2k linear array CCD camera units. The resolution of each camera unit along the circumferential direction is 2048 pixels. That is, the maximum resolution of each sixth of a circle is 2048 pixels. Hence, the precision in the Cartesian space is 0.4 mm. The layout of the six camera units is depicted in Figure 6, which uses a six-camera synchronous scanning system, and the viewing angle of each camera is plotted by purple dash lines. There is a slight overlap between each camera units' viewing angles to ensure no detection dead zone. Besides, the gyroscope is used to identify the circumferential location of the damaged point of the pipeline during the robot's moving.

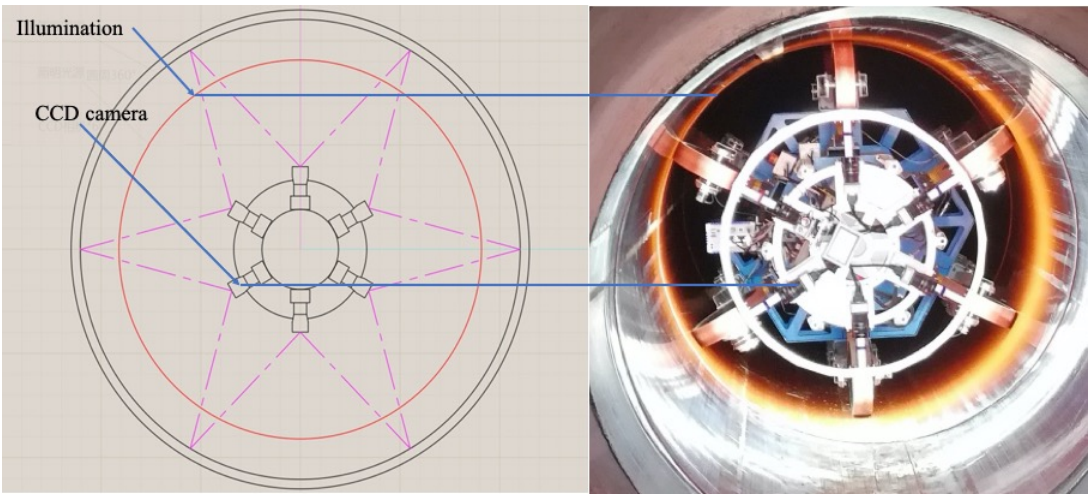

Figure 6. Layout of CCD cameras in inspection system. Note that the illumination indicates the projection of the light from the illuminator onto the wall of the pipeline.

The resolution along the direction of robot motion depends on the performance of the image acquisition system and the robot speed. For example, if the robot speed is 1 m/s, then the operating frequency of the image acquisition system is set at 1 kHz so that the precision can be guaranteed to be 1 mm. The increase in acquisition frequency means that the exposure time will be reduced, so the illumination of the light source must be increased to accommodate the increase of the robot speed.

2.5.2. Image Acquisition System

In the developed system, a data combiner is used to transfer the image information from every three camera units to the CameraLink port of the image acquisition system inside the low-power industrial computer. Therefore, there are two input ports in total, connecting two data combiners and six camera units. The image data is then processed and recorded by the image acquisition system. After the inspection robot finishes a task, data from each camera unit can be restored to image information from the connected port through data processing software. The data size of each camera per meter is 2 MB, so the total data size of six camera units per meter is 12 MB. The industrial computer has a built-in 1-TB solid-state hard disk to ensure sufficient storage space and data storage speed.

2.6. Operations and Functions

After the controller is powered on, the overall system performs a self-check to check that the connection of remote control, motor driver, temperature converter, memory card, and other equipment are working normally. If the system works normally, the LED indicator glows, waiting for the commands from the remote controller. If an abnormality is detected, the buzzer will give an alarm and the LED indicator keeps shining, waiting for troubleshooting.

The system has two operating modes: the manual mode and the autonomous mode. Under the manual mode, after receiving the operation commands from the remote controller, the inspection robot will start its operations until the stopping command is received. Under the autonomous mode, the inspection robot will move forward to the set destination and then return back automatically.

During operation, the inspection robot is adaptive to obstacles. If an obstacle is detected, the inspection robot will automatically stop and move backward three meters, then attempt to pass through it. If it fails to pass through the obstacle three times, it will automatically return.

The overall system has an automatic motor high-temperature protection function. The system detects the temperature of all motors in real time. If it exceeds the set maximum temperature, the inspection robot will stop working and wait for the motor temperature to naturally cool down to the specified value. Besides, the overall system has a data storage function. When the robot is operating, it will record the current set speed, the feedback speed of the four motors, the feedback current of the four motors, the attitude information of the robot, and the mileage of the robot in real time for monitoring and analysis.

3. Field Testing Results on Performance

This section provides the field testing results of the new inspection robot. The entire experiment cycle lasted for several months and was conducted at multiple oil transfer stations to test the inspection robot's capability to operate under different temperatures and humidities. Six aspects of the inspection robot's performance are tested: traction, obstacle-adaptivity, operation endurance, gradeability, visual perception, stability.

3.1. Traction

This testing was conducted at the Daxing Oil Transfer Station (Niufang Village, Daxing District, Beijing, China). When the inspection robot is moving in a horizontally placed pipeline, a pull meter is used to perform multiple drag tests. These tests expected to obtain that the robot could generate a traction force of about 2000 N during normal operation. Part of the testing results are presented in Figure 7.

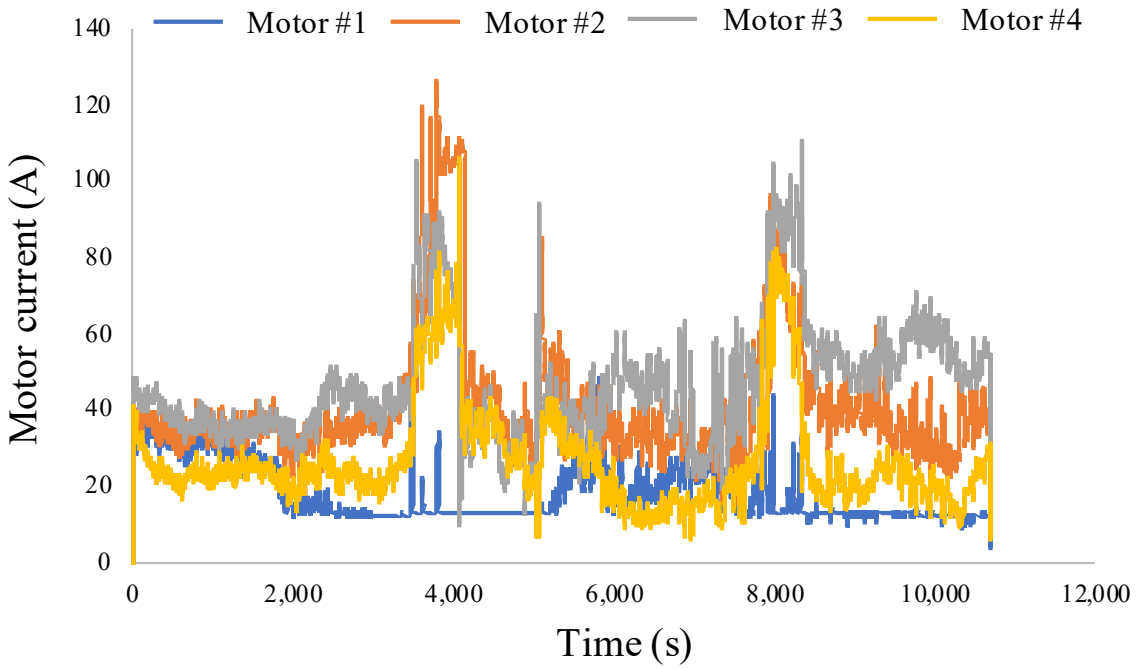

Figure 7. Testing results of traction.

3.2. Obstacle-Adaptivity

When the inspection robot is running in a horizontally placed pipeline, the wooden blocks with various heights are placed inside the pipeline to simulate obstacles or bulges in oil pipelines. The testing results show that the compliance mechanisms enable the inspection robot to successfully pass over the obstacles with 80-mm height inside oil pipelines, as shown in Figure 8.

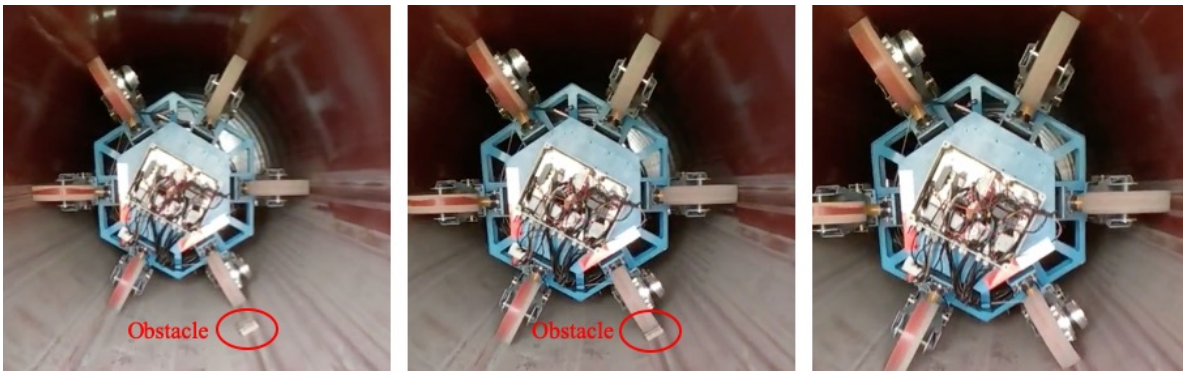

Figure 8. Inspection robot passes over an obstacle.

3.3. Operation Endurance

The previous design of the inspection robot uses a 125-Ah lithium battery, which enables the robot to continuously operate for seven hours and move about 18 km at the Daxing oil transfer station. Compared to this result, the new inspection robot uses a 400-Ah lithium battery to conduct the same testing at the same conditions. After continuously operating for about 31 hours, the operating mileage is about 70 km. Table 2 depicts the testing results of the new inspection robot, where the operating speed keeps at 0.755 m/s, the total weight of the robot is about 300 kg, and the total power of the motors is about 4 kW.

Table 2. Testing results of operation endurance at each timestamp.

No.	Voltage (V)	Time (Hour)	Mileage (km)	Temperature (°C)
1	54.0	0.0	0.0	20
2	52.0	6.5	17.0	20
3	50.0	15.5	33.7	16
4	48.0	20.0	44.5	16
5	46.7	24.0	53	16
6	46.0	26.5	59.5	16
7	44.0	31.5	70.5	16

3.4. Gradeability

In this testing, an 11-meter steel pipe is lifted by a crane to simulate the environment. For each incline angle, the testing is conducted five times. The testing results are depicted in Table 3, where the rate speed is 0.755 m/s.

Table 3. Testing results of gradeability.

No.	Incline Angle (°)	Rate Speed (%)	Slip
1	16	100	No
2	20	100	No
3	30	100	No
4	37	95	No

Figure 9 shows the velocities and currents of four motors during this testing. For better visualization, this paper only shows four motors. In Figure 9, there is almost no change when the incline angle increased from 0° to 37°. Besides, the overall trend of currents is shown as a piecewise function curve with distinct segments.

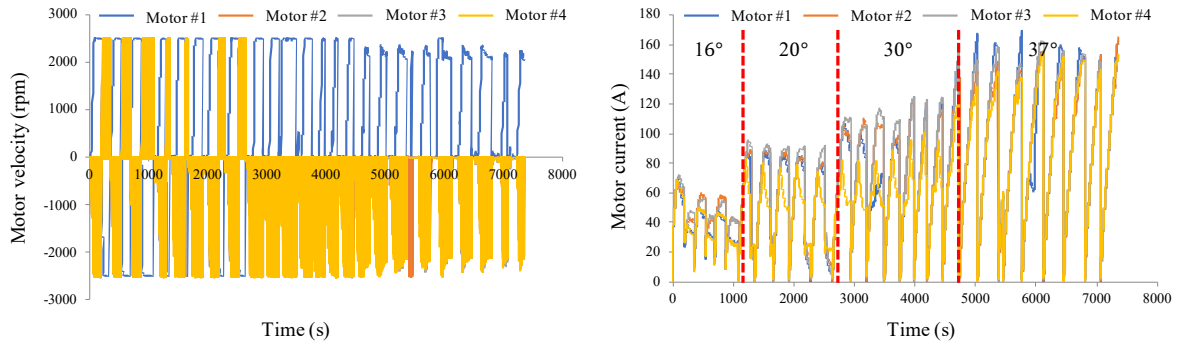

Figure 9. Testing data of gradeability.

3.5. Inspection System

The inspection robot can capture the details of obstacles inside the pipeline. Besides, the pipeline information, pipeline scratches, and other texture details can also be recorded clearly at a running speed of 0.7 m/s. The inspection results are demonstrated in Figure 10. The testing results show that the inspection system can capture a 0.4-mm pipeline scratch caused by mechanical tools during manufacturing.

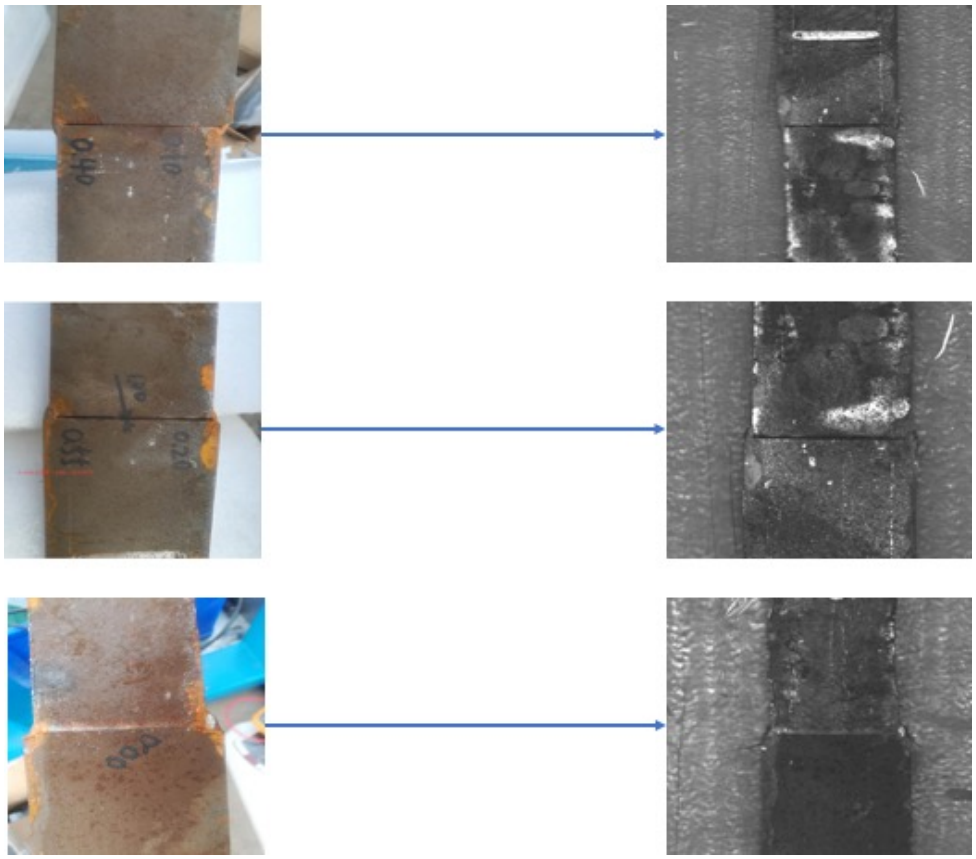

Figure 10. Performance of inspection system when the robot is moving at 0.7 m/s. The left column shows the original objects under normal illumination, and the right column shows the inspection results inside pipelines.

Figure 11 demonstrates that the inspection system can clearly capture the detailed information of each section inside pipelines when the robot is moving, facilitating accurate positioning on the postprocessing of the scratch problems.

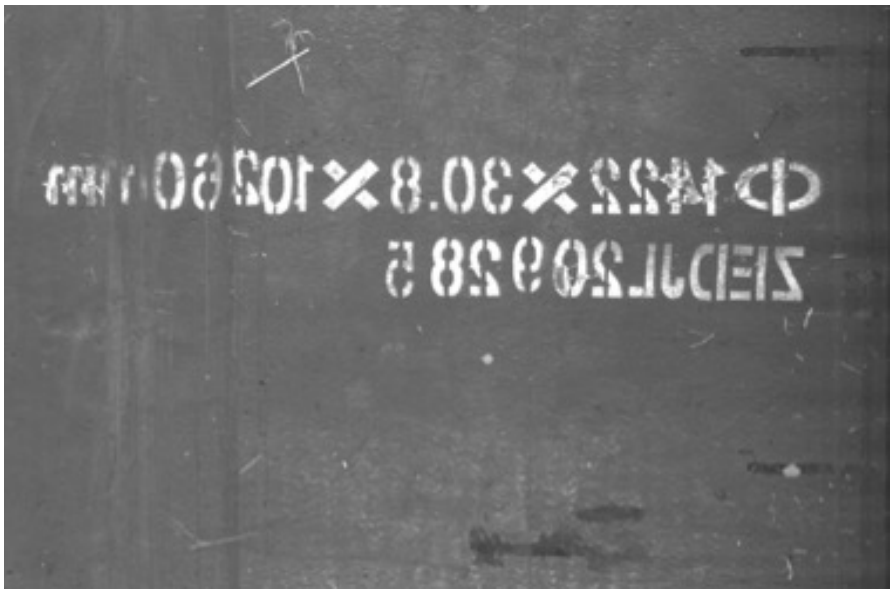

Figure 11. Information captured by inspection system.

3.6. Stability

After the aforementioned performance testing, stability testing was conducted in the severe environment at the Heihe Pipeline Construction Site (Long Town, Heihe City, Heilongjiang Province, China). In an outdoor environment where the temperature is between −15 °C to −20 °C, the testing lasted a week. The testing scene is shown in Figure 12, where the thicknesses of the pipelines (#LY3407358) are 21.4 mm. In this testing, the inspection robot is required to operate in a long pipeline with multiple challenges: horizontal sections, horizontal curved sections, curved pipe climbing sections, and sections with ice. In addition, the inspection robot must have a continuously clear recording inside the pipeline.

Figure 12. Testing scene at the Heihe Pipeline Construction Site.

Figure 13 demonstrates the scene of the robot deployment and operation. There are two climbing sections (14° and 17°) in the testing, as shown in the gyroscope data Figure 14. Overall testing results show the velocities and currents of four motors during this testing (see Figure 15). From these results, the developed inspection robot can generate a uniform motion through the regulation of the motor currents by the control system when facing the aforementioned challenges.

Figure 13. Robot deployment and operation.

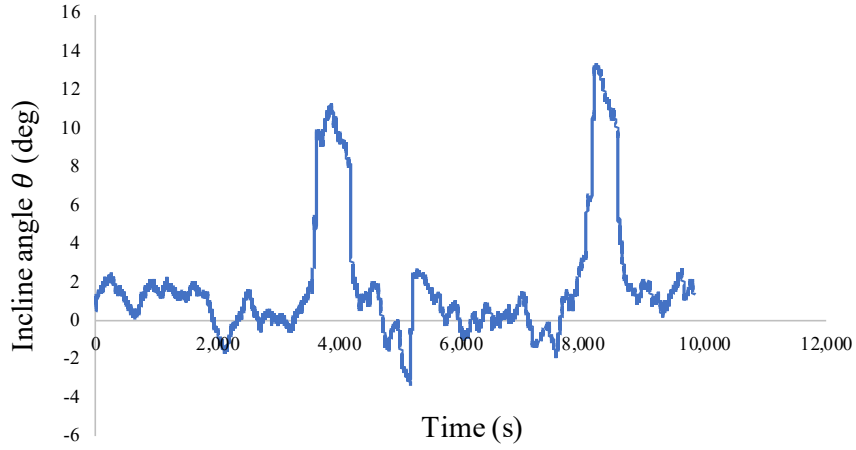

Figure 14. Incline angle detected from gyroscope.

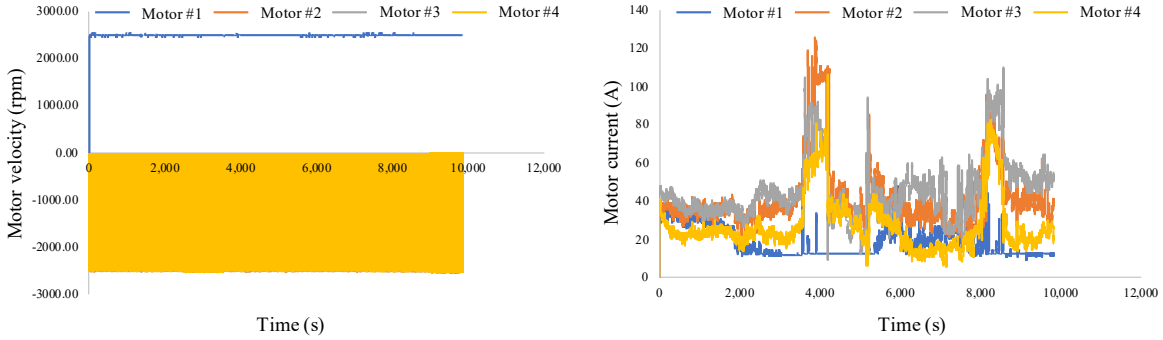

Figure 15. Testing results at the Heihe Pipeline Construction Site.

For the performance of the inspection system in this testing, the information of pipelines and the scratch positions/ranges can be clearly captured, as shown in Figure 16.

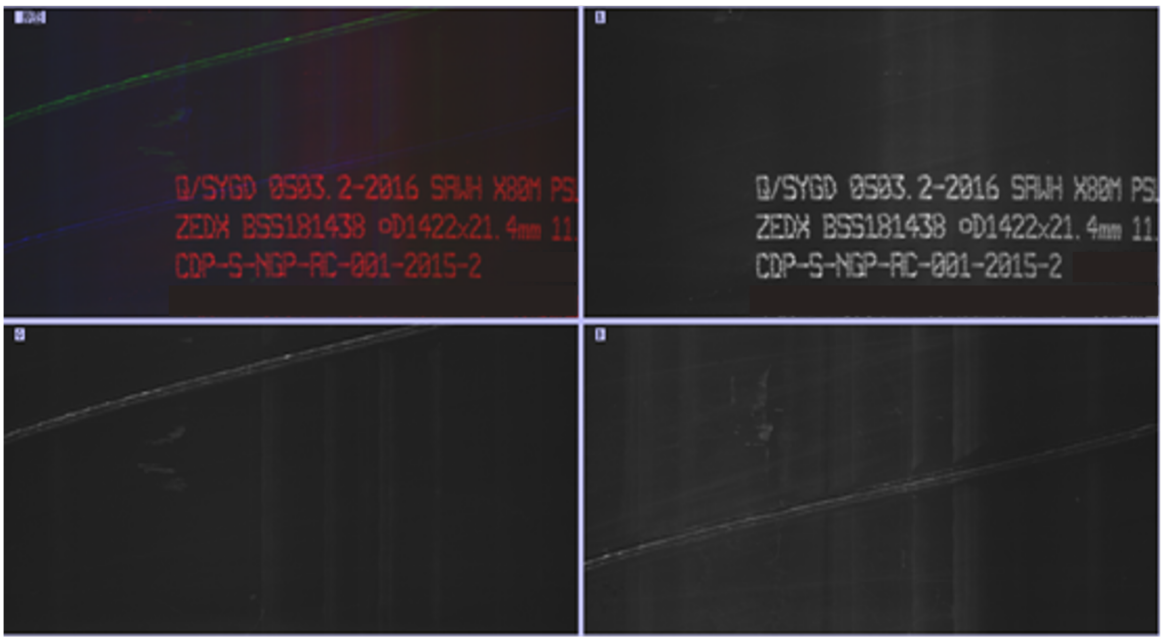

Figure 16. Captured information and scratch in pipelines.

4. Conclusions

This paper presents a newly designed oil pipeline inspection robot for deployment in the standard oil pipelines of the CNPC. The developed inspection robot is based on the previous design, where some efforts are made for improving the performance on six aspects: traction, obstacle-adaptivity, operation endurance, gradeability, visual perception, and stability. A series of field testing was conducted at multiple sites over one year. In addition, the operations in severe environments were also considered: horizontal sections, horizontal curved sections, curved pipe climbing sections, and sections with ice. The testing results show that the developed inspection robot can fulfill the requirements proposed by the CNPC.

In the future, more sensors (e.g., IR sensors and tactile sensors) will be added into the inspection robotic system to satisfy multifunctional purposes in the oil pipeline inspection. Besides, intelligent algorithms based on computer vision will be developed to support online data compression for readable information generation. Furthermore, machine-learning-based diagnoses will also be deployed to accelerate the time-efficiency of data diagnosis and alleviate the burden between the operators and crafted inspectors.

Author Contributions: Conceptualization, R.L. and J.Z.; methodology, H.L.; software, H.L. and P.Z.; validation, H.L., P.Z., and R.L.; formal analysis, H.L.; investigation, H.L.; resources, R.L.; data curation, H.L. and P.Z.; writing–original draft preparation, H.L.; writing–review and editing, R.L.; visualization, H.L.; supervision, R.L.; project administration, R.L.; funding acquisition, R.L. All authors have read and agreed to the published version of the manuscript.

Funding: This research was funded by the Key Research and Development Program of Shanxi Province of China (International Cooperation, 201803D421028, 201903D421051).

Acknowledgments: The authors would like to thank the China National Petroleum Corporation for the assistance and support on the field testing. Besides, the authors would also like to thank the Together Foison (Beijing) Technology Co. Ltd. on the field testing and data collecting.

Conflicts of Interest: The authors declare no conflict of interest.

Abbreviations

The following abbreviations are used in this manuscript:

CNPC	China National Petroleum Corporation
MRO	maintenance, repair, and operations

References

1. China National Petroleum Corporation (CNPC). *2018 Annual Report*; Technical Report; CNPC: Beijing, China, 2018.
2. China National Petroleum Corporation (CNPC). *2018 Corporate Social Responsibility Report*; Technical Report; CNPC: Beijing, China, 2018.
3. Yukawa, T.; Suzuki, M.; Satoh, Y.; Okano, H. Design of magnetic wheels in pipe inspection robot. In Proceedings of the 2006 IEEE International Conference on Systems, Man and Cybernetics, Taipei, Taiwan, 8–11 October 2006; Volume 1, pp. 235–240.
4. Okamoto, J.; Grassi, V.; Amaral, P.F.S.; Pinto, B.G.M.; Pipa, D.; Pires, G.P.; Martins, M.V.M. Development of an autonomous robot for gas storage spheres inspection. *J. Intell. Robot. Syst.* **2012**, *66*, 23–35. [CrossRef]
5. Fei, Y.; Zhao, X.; Wan, J. Motion analysis of a modular inspection robot with magnetic wheels. In Proceedings of the 2006 6th World Congress on Intelligent Control and Automation, Dalian, China, 21–23 June 2006; Volume 2, pp. 8187–8190.
6. Kawaguchi, Y.; Yoshida, I.; Kurumatani, H.; Kikuta, T.; Yamada, Y. Internal pipe inspection robot. In Proceedings of 1995 IEEE International Conference on Robotics and Automation, Nagoya, Japan, 21–27 May 1995; Volume 1, pp. 857–862.

7. Kawaguchi, Y.; Yoshida, I.; Iwao, K.; Kikuta, T. Sensors and crabbing for an in-pipe magnetic-wheeled robot. In Proceedings of IEEE/ASME International Conference on Advanced Intelligent Mechatronics, Tokyo, Japan, 20 June 1997; p. 119.
8. Zhang, Y.; Yan, G. In-pipe inspection robot with active pipe-diameter adaptability and automatic tractive force adjusting. *Mech. Mach. Theory* **2007**, *42*, 1618–1631. [CrossRef]
9. Venkateswaran, S.; Chablat, D. A new inspection robot for pipelines with bends and junctions. In Proceedings of the IFToMM World Congress on Mechanism and Machine Science, Krakow, Poland, 30 June–4 July 2019; pp. 33–42.
10. Hadi, A.; Hassani, A.; Alipour, K.; Askari Moghadam, R.; Pourakbarian Niaz, P. Developing an adaptable pipe inspection robot using shape memory alloy actuators. *J. Intell. Mater. Syst. Struct.* **2020**. [CrossRef]
11. Kwon, Y.S.; Yi, B.J. Design and motion planning of a two-module collaborative indoor pipeline inspection robot. *IEEE Trans. Robot.* **2012**, *28*, 681–696. [CrossRef]
12. Choi, J.Y.; Lim, H.; Yi, B.J. Semi-automatic pipeline inspection robot systems. In Proceedings of the 2006 SICE-ICASE International Joint Conference, Busan, Korea, 18–21 October 2006; pp. 2266–2269.
13. Nassiraei, A.A.; Kawamura, Y.; Ahrary, A.; Mikuriya, Y.; Ishii, K. Concept and design of a fully autonomous sewer pipe inspection mobile robot "kantaro". In Proceedings of the 2007 IEEE International Conference on Robotics and Automation, Roma, Italy, 10–14 April 2007; pp. 136–143.
14. Hoshina, M.; Mashimo, T.; Toyama, S. Development of spherical ultrasonic motor as a camera actuator for pipe inspection robot. In Proceedings of the 2009 IEEE/RSJ International Conference on Intelligent Robots and Systems, St. Louis, MO, USA, 10–15 October 2009; pp. 2379–2384.
15. Dertien, E.; Stramigioli, S.; Pulles, K. Development of an inspection robot for small diameter gas distribution mains. In Proceedings of the 2011 IEEE International Conference on Robotics and Automation, Shanghai, China, 9–13 May 2011; pp. 5044–5049.
16. Gargade, A.; Tambuskar, D.; Thokal, G. Modelling and analysis of pipe inspection robot. *Int. J. Emerg. Technol. Adv. Eng.* **2013**, *3*, 120–126.
17. Liu, Y.J.; Ma, L.; Liu, L.; Tong, S.; Chen, C.P. Adaptive neural network learning controller design for a class of nonlinear systems with time-varying state constraints. *IEEE Trans. Neural Netw. Learn. Syst.* **2019**, *31*, 66–75. [CrossRef] [PubMed]
18. Weng, C.Y.; Yuan, Q.; Suarez-Ruiz, F.; Chen, I.M. A Telemanipulation-Based Human-Robot Collaboration Method to Teach Aerospace Masking Skills. *IEEE Trans. Ind. Inform.* **2019**, *16*, 3076–3084. [CrossRef]
19. Yan, R.J.; Kayacan, E.; Chen, I.M.; Tiong, L.K.; Wu, J. QuicaBot: Quality Inspection and Assessment Robot. *IEEE Trans. Autom. Sci. Eng.* **2018**, *16*, 506–517. [CrossRef]
20. Yan, R.J.; Wu, J.; Lee, J.Y.; Khan, A.M.; Han, C.S.; Kayacan, E.; Chen, I.M. A novel method for 3D reconstruction: Division and merging of overlapping B-spline surfaces. *Comput.-Aided Des.* **2016**, *81*, 14–23. [CrossRef]
21. Weng, C.Y.; Tan, W.C.; Yuan, Q.; Chen, I.M. Quantitative Assessment at Task-Level for Performance of Robotic Configurations and Task Plans. *J. Intell. Robot. Syst.* **2019**, *96*, 439–456. [CrossRef]
22. Wang, H.; Pan, Y.; Li, S.; Yu, H. Robust sliding mode control for robots driven by compliant actuators. *IEEE Trans. Control Syst. Technol.* **2018**, *27*, 1259–1266. [CrossRef]
23. Wang, H.; Zhang, Q.; Xian, J.; Chen, I. Robust Finite-Time Output Feedback Control for Systems with Unpredictable Time-Varying Disturbances. *IEEE Access* **2020**, *8*, 52268–52277. [CrossRef]
24. Liu, L.; Liu, Y.J.; Tong, S. Fuzzy-based multierror constraint control for switched nonlinear systems and its applications. *IEEE Trans. Fuzzy Syst.* **2018**, *27*, 1519–1531. [CrossRef]
25. Zhang, Y.; Liu, L. Adaptive Fault Tolerant Control of Active Suspension Systems With Time-Varying Displacement and Velocity Constraints. *IEEE Access* **2020**, *8*, 10847–10856. [CrossRef]
26. Liu, Y.J.; Zeng, Q.; Tong, S.; Chen, C.P.; Liu, L. Actuator Failure Compensation-Based Adaptive Control of Active Suspension Systems with Prescribed Performance. *IEEE Trans. Ind. Electron.* **2019**, *67*, 7044–7053. [CrossRef]